Wind Energ. Sci. Discuss., doi:10.5194/wes-2017-15, 2017
Manuscript under review for journal Wind Energ. Sci.
Discussion started: 12 April 2017

eawe european academy of wind energy
Open Access WIND ENERGY SCIENCE DISCUSSIONS

Progressive Damage Modeling of Fiberglass/Epoxy Composites with Manufacturing Induced Waves Common to Wind Turbine Blades

Jared W. Nelson[1], Trey W. Riddle[2], and Douglas S. Cairns[3]

[1]SUNY New Paltz, Division of Engineering Programs, New Paltz, NY
[2]Sunstrand, LLC, Louisville, KY
[3]Montana State University, Dept. of Mechanical and Industrial Engineering, Bozeman, MT

Abstract. As part of the Blade Reliability Collaborative, the Montana State University Composites Group has investigated the effects of manufacturing defects. To better understand and predict these effects, various progressive damage modeling approaches were investigated. While the use of damage modeling has increased with improved computational capabilities, they are often performed for worst-case scenarios where damage or defects are replaced with notches or holes. To contribute to the establishment of a protocol understanding and quantifying the effects of these defects, a three-round study was performed using continuum, discrete, and combined damage modeling. This approach relied on a systematically comparing consistency, accuracy and predictive capability for each model. These models were constructed to match the coupons from, and compare the results to, the characterization and material testing study. A standard defect case was chosen and initially used for each modeling approach to perform the qualitative and quantitative comparisons. It was found that while each model was able to show certain attributes, the most consistent, accurate, and predictive model was based on a combined continuum/discrete method. Overall, the results indicate that this combined approach may provide insight into blade performance with known defects when used in conjunction with a probabilistic flaw framework.

1 Introduction

The Department of Energy sponsored, Sandia National Laboratory led, Blade Reliability Collaborative (BRC) has been tasked with developing a comprehensive understanding of wind turbine blade reliability (Paquette, 2012). A major component of this task, to characterize and understand manufacturing flaws commonly found in blades, has been undertaken by the Montana State University Composites Group with focus on two tasks: Flaw Characterization and Effects of Defects. The latter focused on understanding the mechanical performance of materials containing typical flaws and comparing various progressive damage models techniques. As such, different analytical approaches to model progressive damage in flawed composite laminates for consistency, accuracy, and predictive capability. Building upon coupon testing which determined material properties and characterized damage progression, three composite material defect types were investigated: in-plane (IP) waviness, out-of-plane (OP) waviness, and porosity (Nelson et al., 2017). Many different cases for each flaw type were tested allowing for progressive damage quantification, material property definition, and development of many correlation points in this work.

Wind Energ. Sci. Discuss., doi:10.5194/wes-2017-15, 2017
Manuscript under review for journal Wind Energ. Sci.
Discussion started: 12 April 2017

eawe european academy of wind energy
Open Access WIND ENERGY SCIENCE DISCUSSIONS

Two distinct modeling methods have been investigated and compared: Continuum Damage Modeling (CDM), and Discrete Damage Modeling (DDM) (Nelson et al., 2012; Woo et al, 2013). CDM is a "pseudo-representation" that does not model the exact damage, but instead updates the constitutive properties as damage occurs (Kachanov, 1986). This approach assumes that a material is continuous and fills an entire region of space. From this region, the material is broken into representative volume element (RVE) unit cells such that constitutive equations relate the RVE to the entire structure. This allows for the relating of equations to heterogeneous micro-processes that occur during strain of materials locally, and during strain of structures globally, insofar as they are to be described by global continuum variables given their non-homogeneity (Chaboche, 1995). Simply put, actual description of damage is difficult, especially when the damage is on a grain, cell, or micro scale; however, a change in global material response is rather easily noted from the onset of damage. As such, it is often useful to homogenize the material properties of the RVE, a process which is not always feasible when studying composites. In some instances, the two different materials cannot be represented accurately in such a way, especially when damage occurs independently in one of the constituents. Thus, care must be given to the failure modes and types when accounting for the changes in constitutive properties through the damage phases.

Thus, for typical CDM as the model iterates at each strain level, the constitutive matrix is updated to reflect equilibrium damage. Then as damage occurs, the elastic properties are irreversibly affected in ways that are similar to those in a general framework of an irreversible thermodynamic process (Kachanov, 1986). As shown in Figure 1, this takes place by reducing the elastic properties (E_1, E_2, v_{12}, v_{32}, and G_{12}) in the stiffness matrix (C) of the stress-strain relationship. Damage is not directly measurable from this approach, but may be estimated for the continuum by altering observable properties: strength, stiffness, toughness, stability, and residual life. While this method is simple, in some instances two different materials cannot be represented accurately this way and care must be given to the failure modes and types when accounting for the changes in constitutive properties.

$$\begin{Bmatrix}\sigma_{xx}\\ \sigma_{yy}\\ \sigma_{zz}\\ \sigma_{yz}\\ \sigma_{zx}\\ \sigma_{xy}\end{Bmatrix} = \begin{Bmatrix} C_{11} & C_{12} & C_{13} & 0 & 0 & 0 \\ & C_{11} & C_{13} & 0 & 0 & 0 \\ & & C_{33} & 0 & 0 & 0 \\ & & & C_{44} & 0 & 0 \\ & sym & & & C_{44} & 0 \\ & & & & & (C_{12}-C_{12})/2 \end{Bmatrix} \begin{Bmatrix}\varepsilon_{xx}\\ \varepsilon_{yy}\\ \varepsilon_{zz}\\ \varepsilon_{yz}\\ \varepsilon_{zx}\\ \varepsilon_{xy}\end{Bmatrix}$$

Figure 1: Stress-strain relation for a transversely isotropic laminate where the stiffness matrix, *C*, is made up of five elastic constants: E_1, E_2, v_{12}, v_{32}, and G_{12}.

1.1 Continuum Damage Modeling Background

Continuum approaches for composite materials have been well established (Blacketter et al., 1993; Chapman and Whitcomb, 2000; Gorbatikh et al., 2007). In some cases, finite element analysis has been used to account independently for fiber and matrix damage. Chang and Chang (1987) developed a composite laminate in tension with a circular hole where material properties were degraded to represent damage. Failure criteria were defined based on the failure mechanisms resulting from damage: matrix cracking, fiber-matrix shearing, and fiber breakage. A property reduction model was implemented and the

Wind Energ. Sci. Discuss., doi:10.5194/wes-2017-15, 2017
Manuscript under review for journal Wind Energ. Sci.
Discussion started: 12 April 2017

eawe european academy of wind energy
Open Access WIND ENERGY SCIENCE DISCUSSIONS

results were in agreement for seven (7) independent laminates. Later, Chang and Lessard (1991) performed similar work on damage tolerance of laminated composites in compression with a circular hole with similar results. These methods have been utilized for other conditions and have been used to develop a 3D analysis methodology based on the incorporating Hashin failure criteria into a similar logic (Evcil, 2008). By advancing to 3D, the error dropped down to 2.6% from as high as 30%. Additionally, material property degradation models and element failure method have been compared (Tay et al., 2005). While implementing a material property degradation method, as described by references above, it generalizes material and failure may be difficult to visualize. Implementing an element failure method attempts to address this by modification of nodal forces based on micromechanical failure criteria to model damage. Approaches such as these have shown promise when increases in scale are made from coupons all the way to structures; however, prediction beyond initial fiber or matrix failure is questionable. This may be attributed to the oversimplification of the physical damage progression to a continuum model even though each constituent is accounted for independently.

1.2 Discrete Damage Modeling Background

In contrast, a DDM physically models the damage as it occurs through the load profile typically as local failure of the constituents and is considered by many to be more consistent with the physical damage of thermosetting polymer reinforced composites. As noted, a continuum approach relies on representing the damage as a change in material properties, whereas, observed damage is typically local failure of the constituents (matrix and/or fiber). With discrete approaches, constitutive properties do not physically change in a continuum sense and the degradation is a consequence of a local failure. As such, damage is directly modeled as it would occur within a structure. In development of DDM approaches, knowledge *a priori* of the damage location is very helpful, though the result is they are generally computationally more expensive. In addition, more time must also be spent in mesh creation. However, both modeling options have shown promise for modeling composite materials and the specifics of each method utilized are discussed below.

The Virtual Crack Closure Technique (VCCT) is a DDM that has been used with success for delamination growth in composite materials and structures. VCCT calculates the fracture energy at the crack tip by calculating the energy required to close the crack (Krueger, 2004). The work required to bring nodes together is used to calculate strain energy release rates. This technique is particularly useful for establishing or confirming critical strain energy release rates in either Mode I or II, G_{Ic} and G_{IIc}, respectively. The authors have used this for delamination growth modeling, but VCCT is a relatively mature procedure, the results are not presented.

Several techniques for discrete modeling exist such that crack development and path may be modeled. Originally, discrete models had discrete crack propagation and would be followed by a re-meshing with the new geometry. This cycle is repeated until ultimate failure has been reached based on one of several crack propagation criteria (Bouchard, et al., 2000). The discontinuity created by the crack can make re-meshing difficult and extended finite element modeling (XFEM) allows for a crack to propagate without having to re-mesh at each step (Areias and Belytschko, 2005).

Wind Energ. Sci. Discuss., doi:10.5194/wes-2017-15, 2017
Manuscript under review for journal Wind Energ. Sci.
Discussion started: 12 April 2017

The continual increase in computational availability has allowed for finer mesh refinement and paved the way for the use of cohesive elements for modeling laminated composites without an initial crack (Karayez et al., 2012). These zero thickness elements are useful with laminated composites because they may be placed between layers or fibers. A bi-linear traction-separation criterion is employed such that the element has a linear stiffness response until the maximum traction point is reached and damage is initiated. Then, the second portion of the bi-linear response estimates the damage evolution up to failure where separation occurs and the element is deleted. It is not necessary to know the bi-linear response as it may be developed iteratively using experimental/analytical correlation. While this method is computationally expensive due to extensive number of elements needed, this method has been shown to effectively model crack propagation.

2 Systematic Approach Methodology

A systematic approach was employed to compare different modeling methods discussed (Figure 2). For each different model method, an initial IP wave case was utilized and the resulting correlation was deemed acceptable or unacceptable. If a method was deemed acceptable for this initial case, additional flaw geometries were analyzed. Thus, fully acceptable modeling methods were able to predict and match flawed material response for multiple flaw types utilizing unflawed material properties and flaw geometries. It is worth noting that a qualitative/quantitative approach was utilized similar to that utilized by Lemanski et al., though strains at peak stress were also considered (Lemanski, 2013). Acceptable models correlated well both qualitatively, by matching failure location and shape, and quantitatively, by matching initial stiffness and peak stress at failure strain. For each different model method, flaw complexity was increased, starting with a consistent unflawed case and initial IP wave case, until the correlation was deemed acceptable or unacceptable. Acceptable modeling methods were able to predict and match flawed material response for multiple flaw types utilizing unflawed material properties and flaw geometries.

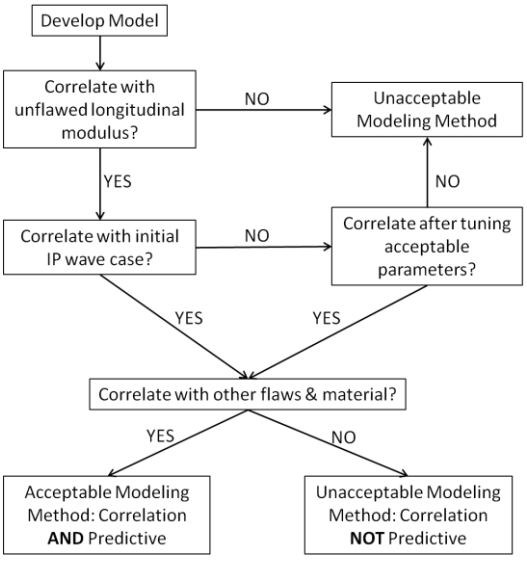

Figure 2: Systematic flow of approach to determine acceptability of each model.

Wind Energ. Sci. Discuss., doi:10.5194/wes-2017-15, 2017
Manuscript under review for journal Wind Energ. Sci.
Discussion started: 12 April 2017

As shown in Figure 2, if correlation was not achieved by a model at any point during the systematic increase in flaw complexity, the model was deemed unacceptable and no additional flaw geometries were tested. Unless otherwise noted, the increase in flaw complexity in each case went from unflawed controls to porosity to the IP wave baseline case to the initial OP wave case, and then to other IP and OP geometries. Acceptable models were able to accurately and consistently predict each of these cases, and with this consistent systematic approach, the different techniques were able to be compared easily.

Acceptance criteria was defined to allow for consistent analysis at each decision point of Figure 2. First, a qualitative assessment was performed and correlation was deemed acceptable if strain accumulation and damage progression visually matched the testing results. While this assessment method may seem crude, it allows for quick analysis of several key factors including an energy comparison. An energy comparison ensured that the energy was conserved between the strain energy available and energy dissipated. Qualitative comparison of the unrecoverable energy, or area under the curves, was deemed sufficient as models that do not conserve energy were evident and were not considered acceptable. While conservation may be inherent in finite element analysis, it was shown that this comparison gave rapid indication when a model was unrealistic as seen with the non-linear shear approach. As such, qualitative assessment provided a rapid go/no-go gage.

If the qualitative criteria were met, a quantitative assessment was performed. First, the strain at peak stress was compared and deemed acceptable if it was within 10% of testing results. If acceptable, peak stress was compared and also deemed acceptable if it was within 10% of testing results. These areas of quantitative acceptability are shown in Figure 3. While these acceptance criteria were beyond the variability noted in the testing, if these criteria were outside 10%, but within 20%, correlation was considered moderate. It is important to note that this consideration was only made for correlation with other flaws and/or materials after acceptable correlation had been achieved for the initial IP wave case. As such, models were considered predictive if correlation was achieved with these other cases utilizing the same input parameters as the initial IP wave case.

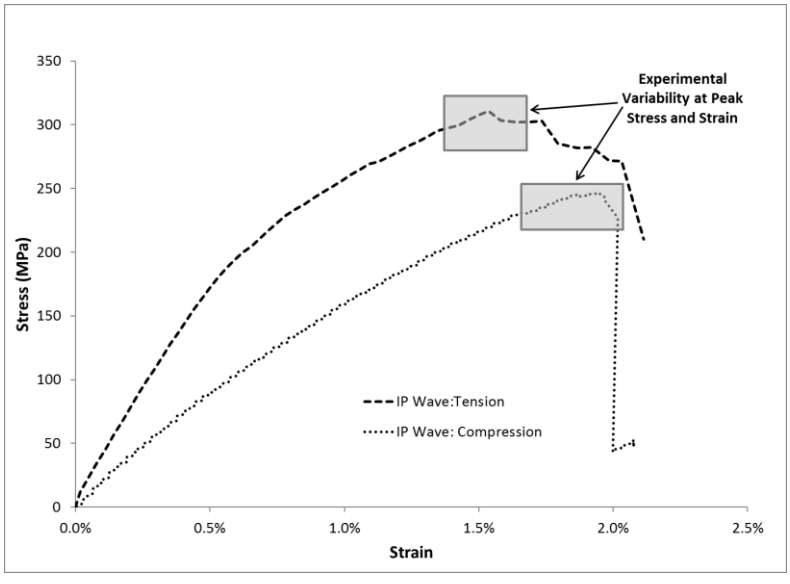

Figure 3: Tension and compression response of IP Wave 1 utilized for baseline correlations with associated experimental variability.

Wind Energ. Sci. Discuss., doi:10.5194/wes-2017-15, 2017
Manuscript under review for journal Wind Energ. Sci.
Discussion started: 12 April 2017

eawe european academy of wind energy
Open Access WIND ENERGY SCIENCE DISCUSSIONS

3 Modeling Techniques

Several different modeling approaches were utilized and each is outlined below. For each approach, a baseline linear elastic model was used and the geometry was set up to match the intended coupon size (100 mm x 50 mm) established during material testing. To determine if initial correlations were reasonable, 2D models (Figure 4) were generated with both unflawed and IP wave geometries, with quadrilateral, plane stress shell elements (S4R), in Abaqus where each element was generated to be consistent with the nominal fiber tow width (1.0 mm). The initial IP wave modeled had an amplitude (A) of 3.8 mm, a wavelength (λ) of 47.6 mm, and average off-axis fiber angle of 28.7°. Local coordinate systems were defined for the elements oriented to form the wave such that the fiber direction remained consistent through the wave, and the material properties were modeled to correctly match these properties. Displacement and boundary conditions were applied at the top and bottom, respectively, to match the testing conditions and as such, full field calculations were set to match the testing data for load-displacement and stress-strain correlations. Elastic material properties and damage progression noted in testing were utilized, as shown in Table 1. The geometry shown in Figure 4 was utilized for all of the initial IP wave modeling efforts.

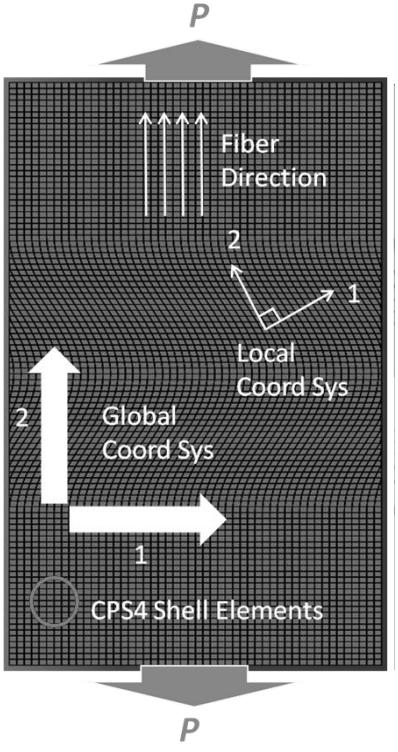

Figure 4: Representation of model and references used for IP wave model.

Table 1: Empirical material properties utilized in Progressive Damage Analysis.

	E_1	E_2	v_1	G_{12}	G_{13}	G_{23}
Tension (GPa)	40.6	16.3	0.27	16.8	16.8	16.8
Compression (GPa)	38.4	14.4	0.28	14.4	14.4	14.4

Wind Energ. Sci. Discuss., doi:10.5194/wes-2017-15, 2017
Manuscript under review for journal Wind Energ. Sci.
Discussion started: 12 April 2017

eawe european academy of wind energy
Open Access WIND ENERGY SCIENCE DISCUSSIONS

Several assumptions were made to simplify this modeling effort. First, it was assumed that all fibers were parallel and uniform in the intended direction with reference to the width-wise edge, including through the IP wave. It was also assumed that all the fibers, for both the unflawed and IP wave geometries, were parallel and aligned through the thickness. These assumptions greatly simplified the modeling approach even though they were a possible source of the variation noted within the testing. In addition, perfect bonding between the layers was assumed. Three distinct CDM and one DDM techniques were utilized to determine consistency, accuracy, and predictive capability compared to the testing results.

3.1 Hashin-based Progessive Damage

First, the Abaqus built-in a Progressive Damage and Failure for Fiber-Reinforced Materials (Analysis User's Manual v6.12, 2012) that is intended to be used for elastic-brittle, anisotropic materials based on the Hashin failure criteria was utilized. In this case, the elastic response is defined as a linear elastic material with a plane stress orthotropic material stiffness matrix. However, damage initiation must also be defined for the four included mechanisms: fiber tension, fiber compression, matrix tension, and matrix compression. Once damage is initiated in one or more of these mechanisms, elemental properties are degraded according to the defined damage evolution response:

Fiber tension ($\hat{\sigma}_{11} \geq 0$):
$$F_f^t = \left(\frac{\hat{\sigma}_{11}}{X^T}\right)^2 + \alpha\left(\frac{\hat{\tau}_{12}}{S^L}\right)^2 \quad (1)$$

Fiber compression ($\hat{\sigma}_{11} < 0$):
$$F_f^c = \left(\frac{\hat{\sigma}_{11}}{X^C}\right)^2 \quad (2)$$

Matrix tension ($\hat{\sigma}_{22} \geq 0$):
$$F_m^t = \left(\frac{\hat{\sigma}_{22}}{Y^T}\right)^2 + \left(\frac{\hat{\tau}_{12}}{S^L}\right)^2 \quad (3)$$

Matrix compression ($\hat{\sigma}_{22} < 0$):
$$F_m^c = \left(\frac{\hat{\sigma}_{22}}{2S^T}\right)^2 + \left[\left(\frac{Y^C}{2S^T}\right)^2 - 1\right]\frac{\hat{\sigma}_{22}}{Y^C} + \left(\frac{\hat{\tau}_{12}}{S^L}\right)^2 \quad (4)$$

where X^T is the longitudinal tensile strength, X^C is the longitudinal compressive strength, Y^T is the transverse tensile strength, Y^C is the transverse compressive strength, S^L is longitudinal shear strength, S^T is transverse shear strength, α is a shear stress contribution coefficient that determines contribution to fiber tensile initiation, and $\hat{\sigma}_{11}$, $\hat{\sigma}_{22}$, $\hat{\tau}_{12}$ are stress tensor components where the nominal stress is modified with a damage operator, M:

$$M = \begin{bmatrix} \frac{1}{1-d_f} & 0 & 0 \\ 0 & \frac{1}{1-d_m} & 0 \\ 0 & 0 & \frac{1}{1-d_s} \end{bmatrix} \quad (5)$$

Wind Energ. Sci. Discuss., doi:10.5194/wes-2017-15, 2017
Manuscript under review for journal Wind Energ. Sci.
Discussion started: 12 April 2017

eawe european academy of wind energy
Open Access WIND ENERGY SCIENCE DISCUSSIONS

where d_f, d_m, and d_s are damage variables for fiber, matrix, and shear damage, respectively, derived from the damage variables of the stress scenarios noted in the four mechanisms listed above. where d_f, d_m, and d_s are damage variables for fiber, matrix, and shear damage, respectively, derived from the damage variables of the stress scenarios noted in the four mechanisms listed above. As damage progresses, the model assesses the displacements which are used to determine these damage variables using the damage law for each fiber, matrix, and shear:

$$d = \begin{cases} 0 & \text{if no damage} \\ \dfrac{\delta_{eq}^{f}(\delta_{eq} - \delta_{eq}^{0})}{\delta_{eq}(\delta_{eq}^{f} - \delta_{eq}^{0})} & \text{from damage onset to full damage (complete failure)} \end{cases} \tag{6}$$

where δ_{eq}^{0} is the equivalent displacement for damage initiation, δ_{eq} is the equivalent displacement calculated by the code for each of the four mechanisms, and δ_{eq}^{f} is the equivalent displacement at which the material is fully damaged. It is worth noting that all equivalent displacements are calculated using the definition of strain from the characteristic length and strains determined in the model. If the modified stress tensor components meet the criteria for any of the four mechanisms, then damage is initiated. The damage variables become non-zero, the damage operator, M, modifies the nominal stress, and appropriate stiffness degradation begins. Instead of continuing with the stiffness matrix of a plane stress orthotropic material, the degraded material response is then calculated:

$$\sigma = \mathrm{C_d}\varepsilon \tag{7}$$

where:

$$\mathrm{C_d} = \frac{1}{D}\begin{bmatrix} (1-d_f)E_1 & (1-d_f)(1-d_m)\nu_{21}E_1 & 0 \\ (1-d_f)(1-d_m)\nu_{12}E_2 & (1-d_m)E_2 & 0 \\ 0 & 0 & (1-d_s)GD \end{bmatrix} \tag{8}$$

and:

$$D = 1 - (1-d_f)(1-d_m)\upsilon_{12}\upsilon_{21} \tag{9}$$

where, again, d_f , d_m, and d_s each reflected the current state of fiber, matrix, and shear damage, respectively, E_1, E_2, and G are the directional and shear moduli of elasticity, respectively, and ν_{12} and ν_{21} are Poisson's ratios. Unidirectional Damage initiation and Strain Energy Release Rates used for the PDA are shown in Table 2 and was generated during the same independent testing as in Table 1.

Table 2: Damage initiation and evolution parameters utilized in Progressive Damage Analysis.

Property	X^T	X^C	Y^T	Y^C	S^L	S^T	G^C_{Lt}	G^C_{Lc}	G^C_{Tt}	G^C_{Tc}
Value	990	582	60	162	112	124	16.0	16.9	39.9	45.1
Units	MPa					kN/mm				

Wind Energ. Sci. Discuss., doi:10.5194/wes-2017-15, 2017
Manuscript under review for journal Wind Energ. Sci.
Discussion started: 12 April 2017

eawe european academy of wind energy
Open Access WIND ENERGY SCIENCE DISCUSSIONS

3.2 User-defined Subroutine

Next, a user-defined subroutine was employed with a combined maximum stress/strain user specified failure criteria where the standard input file builds and meshes the model, while the user subroutine checks for damage at each step (Chang and Chang, 1987; Chang and Lessard, 1991). If damage is detected, the material properties were adjusted or the loop is stopped if ultimate failure has occurred. If damage is detected, but not ultimate failure, the material properties are degraded depending on the type of failure as outlined in Table 3.

Table 3: Progressive Damage Analysis degradation for User Defined Criteria

Material Failure Type	Elastic Property Adjustments for Each Failure Type				Notes
No Failure	E_x	E_y	v_{xy}	G_{xy}	Full properties.
Matrix Cracking Damage	E_x	0	0	G_{xy}	Used in tensile and compressive cases.
Fiber-Matrix Damage	E_x	E_y	0	0	Fiber compresses & matrix cracks; used in compression only.
Fiber Failure	0	0	0	0	Fiber buckles or breaks; all properties drop to zero.
Combined Matrix Cracking & Fiber-Matrix Damage	E_x	0	0	0	Fiber is still intact and able to carry some longitudinal load.
Combined Matrix Cracking Damage & Fiber Failure	0	0	0	0	All properties drop to zero.
Combined Fiber-Matrix Damage & Fiber Failure	0	0	0	0	
All Combined Failure Modes	0	0	0	0	

To determine the failure values, user-defined failure criteria integrating both maximum stress and strain criteria were implemented into the subroutine. A modified maximum stress failure criterion was implemented with the inclusion of a maximum strain criteria to accurately model ultimate fiber failure. As such, matrix cracking damage was estimated by:

$$\left(\frac{\sigma_{22}}{Y_T}\right)^2 + \left(\frac{\tau_{12}}{S_T}\right)^2 = 1 \tag{10}$$

where σ_{22} and Y_T are transverse stress and transverse strength, respectively, and τ_{12} and S_T are shear stress and strength, respectively. It must be noted that this same equation was utilized for both tensile and compressive cases, and the associated material properties are changed for each case. While the fiber-matrix compression damage case appeared to be necessary only in compression loading cases, with the given geometries these failure criteria were utilized in both tensile and compressive cases:

$$\frac{\sigma_{11,C}}{Y_C} + \frac{\tau_{12}}{S_T} = 1 \tag{11}$$

where $\sigma_{11,C}$ and Y_C are fiber compressive stress and strength, respectively. Finally, two different equations were utilized depending on whether fiber failure is in tension or compression, respectively:

Wind Energ. Sci. Discuss., doi:10.5194/wes-2017-15, 2017
Manuscript under review for journal Wind Energ. Sci.
Discussion started: 12 April 2017

$$\frac{\varepsilon_{11,T}}{\bar{\varepsilon}_T} = 1 \tag{12}$$

$$\frac{\sigma_{22,C}}{X_C} = 1 \tag{13}$$

where $\varepsilon_{11,T}$ and $\bar{\varepsilon}_{11,T}$ were calculated for ultimate tensile strain and compressive stress, respectively. Utilization of the maximum strain criterion in tension was based on the consistency of strain at failure of these materials as determined in the testing. Integration of this criterion was a fundamental motivation in utilizing this user-defined technique.

Thus, at each increment the subroutine ran through these failure criteria equations that utilize the stress and strain data of that increment. Resulting values of these equations range from zero (0) to one (1) with failure occurring when the value was equal to one (1). As the failure indices were calculated to be one (1), failure has occurred in that element and the material properties were adjusted based on the failure type as noted in Table 3. For example, if a matrix failure occurred, the failure indices included in the user subroutine calculated that Failure Value #1 became equal to one (1). As a result, the elastic properties for that element only include E_x and G_{xy} as these are fiber dominated. The loop continued with the degraded properties until fiber failure or a combination of failures occurred resulting in no material properties for that element.

3.3 Non-linear Shear Model

Based on the shear between the fiber tows in the wavy area, it was deemed that a non-linear constitutive law needed to be developed for the bulk material using a user defined material subroutine (UMAT) in Abaqus. Using the tabulated shear stress-strain relationship (Figure 5, left), the shear stress and tangential modulus were calculated by the subroutine and updated into the material card of the model. Shear stress-strain from the actual materials used for these tests data was then utilized in the UMAT and a zero-stiffness condition was approximated to ensure model convergence.

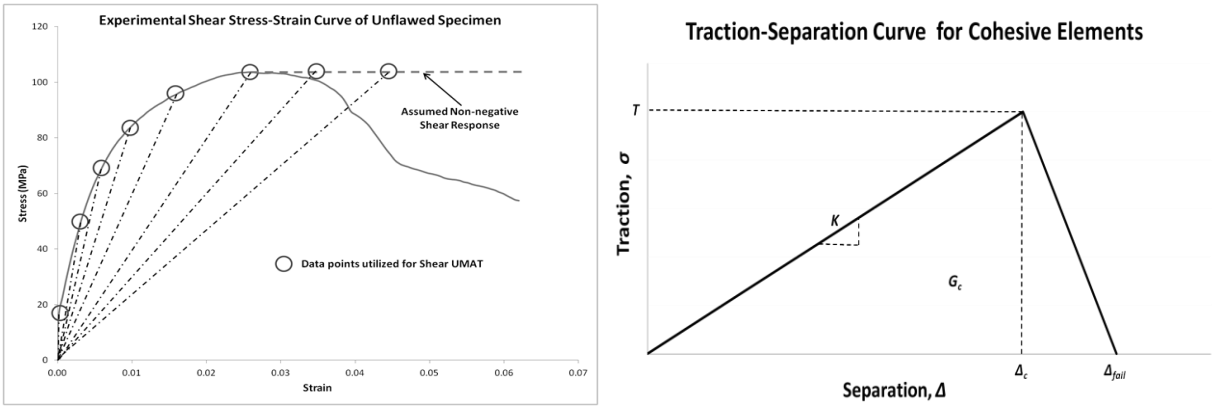

Figure 5: Tabulated points from empirical shear stress-strain relationship for UMAT (left); and representation of bi-linear traction-separation response for a cohesive element (right).

Wind Energ. Sci. Discuss., doi:10.5194/wes-2017-15, 2017
Manuscript under review for journal Wind Energ. Sci.
Discussion started: 12 April 2017

eawe european academy of wind energy
Open Access WIND ENERGY SCIENCE DISCUSSIONS

3.4 Cohesive Zone Model

To model damage progression discretely, cohesive elements are typically utilized based on a cohesive law relating traction to separation across the interface (Karayev et al., 2012; Lemanski et al., 2013). Zero thickness elements with specific bi-linear traction-separation criteria (Figure 5, right) were placed between the fiber tows. While previous convention was to utilize cohesive elements only in specific areas, predefining the crack path, computational availability has made it conceivable to place cohesive elements throughout the model. Thus, damage and crack progression may occur virtually anywhere in the model where the stress state indicates rather than where the user has placed these elements.

3.5 Combined Non-linear Shear and Cohesive Zone Model

A bi-linear criterion was used as shown in Figure 5 where the initial stiffness, K, of the cohesive element is linear up to the damage initiation point at critical separation, Δ_c. From this point to the failure separation, Δ_{fail}, the slope estimates the damage evolution of each the cohesive element up to failure. The traction-separation criterion is met for a specific cohesive element and a separation occurs resulting in crack propagation and element deletion. As such, damage progression can be modeled discretely. Based on the inexact ability to determine these parameters, they must be adjusted in an iterative approach resulting in multiple model runs to establish reasonable analytical/experimental correlation. Such parametric studies were performed to ensure that these cohesive properties do not impact the stiffness and response of the surrounding material in ways other than those intended.

Based on the results of the individual methods noted above, a non-linear shear CDM was combined with a DDM using cohesive elements. As discussed below, in both cases, the models seemed to capture portions damage progression, while each lacked the exact progression observed in the testing. It was believed that by combining them, the interaction of the two model types would result in a consistent, accurate, and predictive analytical tool.

4 Results & Discussion

Several analytical models were created, run, and correlated to responses outlined in the testing effort and modified to improve correlation. Flaw complexity and computational difficulty were both increased within and between model types, respectively. While correlation was found rather easily in some cases, other cases required significant modification, or tuning, of input parameters. In some cases, correlation could be achieved by small amounts of acceptable parameter tuning. These acceptable tuning parameters, in most cases, were adjusted to assist with convergence, and the effects on the model, or element section, were able to be tracked. In other cases, material properties were modified as a final approach to attempt correlation. Adjustment of these types of parameters was unacceptable tuning, and while correlation may have been achieved, the model type was a failure for unbiased prediction efforts. It must be noted that these unacceptable tuning methods were performed only to better understand the effects on modeling and are not included. Below, each case is presented, a discussion is offered for each correlation, and either modification of input parameters is justified or the model type is found to be inaccurate.

Wind Energ. Sci. Discuss., doi:10.5194/wes-2017-15, 2017
Manuscript under review for journal Wind Energ. Sci.
Discussion started: 12 April 2017

eawe european academy of wind energy
Open Access WIND ENERGY SCIENCE DISCUSSIONS

4.1 Qualitative Damage Progression Comparison

For each modeling technique a qualitative analysis, and then a quantitative analysis, was performed. Images were analyzed and qualitative comparisons were made through the damage progression as exemplified in Figure 6. In Figure 6 (left), it may be seen that failure occurred first at the edges where fibers were discontinuous at low loading. As the load increased, damage accumulation may be noted in the fiber misalignment section with shear failure occurring in the matrix as the fibers straightened due to tensile elongation (Figure 6, right). As may be expected, the failure areas are cleaner and less complex for the models due to uniformity and symmetry of the modeled specimen. Notably, the qualitative correlation was quite consistent through the initial, low-load portion of each analysis where shear load increased significantly through the wavy section for all the modeling techniques.

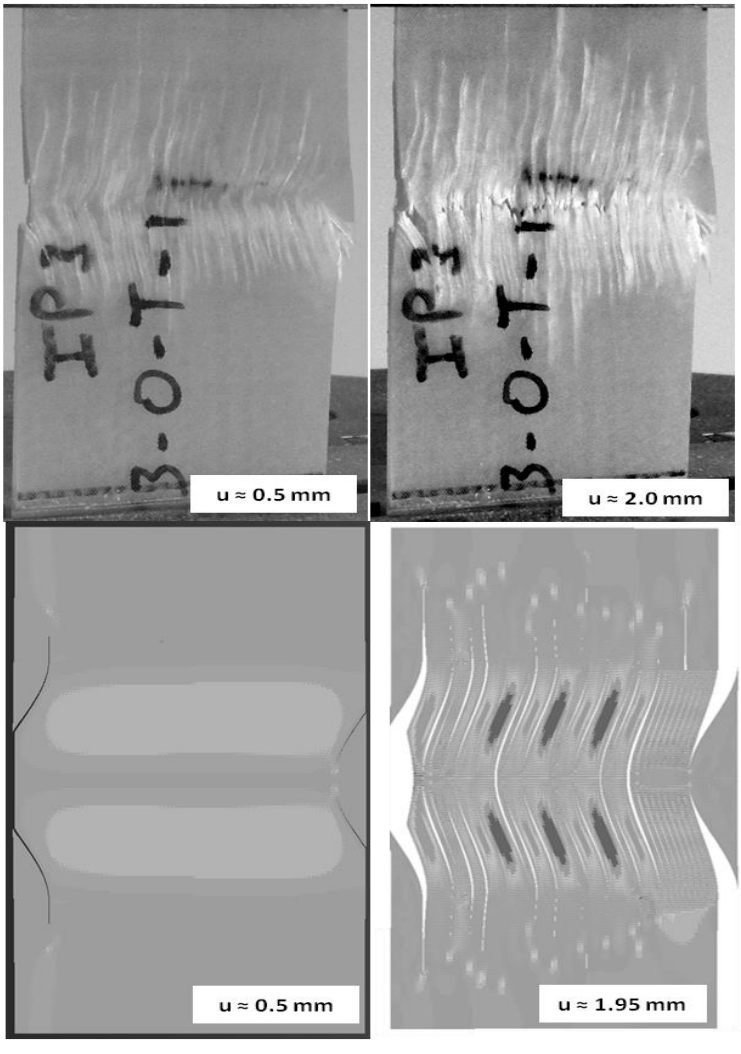

Figure 6: Comparison of damage between experimental (above) and analytical (below) showing onset-to-final damage left-to-right, respectively.

Wind Energ. Sci. Discuss., doi:10.5194/wes-2017-15, 2017
Manuscript under review for journal Wind Energ. Sci.
Discussion started: 12 April 2017

eawe european academy of wind energy
Open Access WIND ENERGY SCIENCE DISCUSSIONS

4.2 Quantitative Material Response Comparison

For each technique, stress-strain relationships were generated using the same method of far-field strain utilized during experimentation (Figure 7). Where response appeared to be similar from the qualitative analysis, the differences in the responses from modeling techniques is clearly quantified. To summarize the comparisons, Table 4 outlines the graded results of each model technique while noting both the input parameters and the parameters acceptable for tuning. Following the systematic approach, a modulus check (MC) was performed first for all cases. Next, a CDM approach where material properties were degraded based on amount of included air was performed for porosity and acceptable correlation (A) was achieved in tension. However, while the results appeared reasonable in compression, experimental data was not sufficient to perform correlation (R). In order to consider fiber waviness, each model was checked for the same initial IP wave case before moving on to consider other waves and/or materials if acceptable correlation was found. Finally, no addition cases were run for a model if correlation for this initial case was found to be unacceptable (U). This was found to be the case for the user-defined failure criteria, non-linear shear, and cohesive element models which showed poor correlation. However, the Hashin failure criteria model and the combined model were found to have good correlation, resulting in further testing. The results of each method are discussed below.

A linear elastic model was modified to include the Hashin failure criteria built into. First, a model was created and utilized for porosity before the initial IP wave case was run. For porosity, the criteria for acceptable and marginal correlations were achieved for tension and compression, respectively. Given these results and the predictive ability when varied for different amounts of porosity, the approach was deemed acceptable and further investigation was not performed. For the initial IP wave case, regions of acceptability were noted and was improved when the acceptable parameters (damage initiation, evolution, and stabilization) were adjusted (Figure 7). Once the initial model was tuned, additional wave and material cases were run as indicated in Table 4 and found to be predictive in all cases indicating the promise of this method.

Wind Energ. Sci. Discuss., doi:10.5194/wes-2017-15, 2017
Manuscript under review for journal Wind Energ. Sci.
Discussion started: 12 April 2017

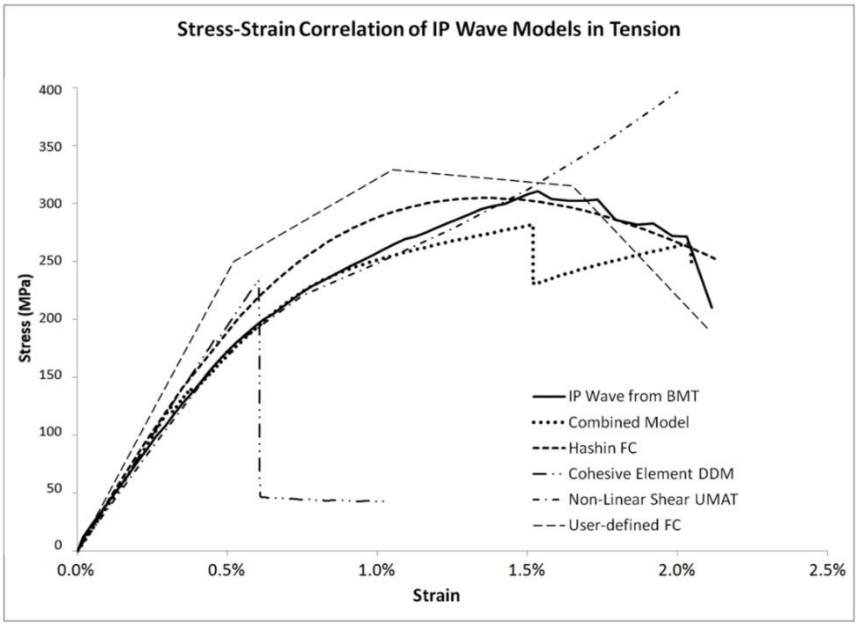

Figure 7: Resulting stress-strain curves of each model compared to experimental results.

Table 4: Summary of results of each model for acceptability with input and tuned parameters identified.

			UNFLAWED		POROSITY		IP WAVE		OP WAVE		ADDITIONAL WAVES AND MATERIAL		INPUT PARAMETERS	TUNED PARAMETERS (ACCEPTABLE)
Model Type	Model	Effects of Defects Round	Tension	Comp	Tension	Comp	Tension	Comp	Tension	Comp	Tension	Comp		
CDM	Linear Elastic	1	MC	MC	NR	NR	NR	NR	NR	NR	NR	NR	ELASTIC PROPERTIES	NONE
	Linear Elastic w/ Hashin Failure Criteria	1	MC	MC	A	M	A	M	A	R	A,M	R	ELASTIC PROPERTIES & DAMAGE INITIATION, EVOLUTION, &	DAMAGE INITIATION, EVOLUTION, & STABILIZATION
	Subroutine w/ User-defined Damage Criteria	2	MC	MC	NR	NR	U	U	NR	NR	NR	NR	ELASTIC PROPERTIES, REDUCED PROPERTIES, & FAILURE CRITERIA	REDUCED PROPERTIES
	Non-Linear Shear	2	MC	MC	NR	NR	U	U	NR	NR	NR	NR	ELASTIC PROPERITES & STRESS-STRAIN FROM UNFLAWED SHEAR RESPONSE	SUBTLE CHANGES TO STRESS-STRAIN
DDM	Cohesive Elements between Tows	2	MC	MC	NR	NR	U	U	NR	NR	NR	NR	ELASTIC PROPERTIES & COHESIVE TRACTION-SEPARATION	COHESIVE TRACTION-SEPARATION
Combined	Non-Linear Shear w/ Cohesive Elements between Tows	3	MC	MC	NR	NR	A	A	A	R	A	A,R	ELASTIC PROPERTIES, STRESS-STRAIN FROM UNFLAWED SHEAR RESPONSE, & COHESIVE TRACTION-SEPARATION	SUBTLE CHANGES TO STRESS-STRAIN & COHESIVE TRACTION-SEPARATION

KEY:
A = ACCEPTABLE CORRELATION (visual correlation and within 10% of Strain at Peak Stress while also within 10% of Peak Stress)
M = MODERATE CORRELATION (visual correlation but marginal quantitative acceptance criteria)
U = UNACCEPTABLE CORRELATION (unacceptable visual and/or quantitative correlation)
R = MODEL RUN BUT NOT CORRELATED (insufficient test data available)
NR = MODEL NOT RUN (due to unacceptable initial case or acceptable overall method)
MC = INITIAL MODULUS CHECK (stiffness of model within 5% of test)

Wind Energ. Sci. Discuss., doi:10.5194/wes-2017-15, 2017
Manuscript under review for journal Wind Energ. Sci.
Discussion started: 12 April 2017

eawe european academy of wind energy
Open Access WIND ENERGY SCIENCE DISCUSSIONS

While the Hashin failure criteria successfully met the acceptance criteria, it did not exactly match the experimental material response particularly from 0.5-1.5% strain (Figure 7). In order to offer the user more control to improve the modeling of the material response, the subroutine with user-defined failure criteria was used. After significant tuning of the material property degradation scheme, sufficient correlation was not achieved and the response showed a greater difference than the Hashin failure criteria in the area of interest. As such, this approach was deemed unacceptable, as noted in Table 4 and no further attempts at correlation were attempted.

Both a CDM using a non-linear shear response and a DDM using cohesive elements, respectively, were attempted independently. While neither case was able to accurately model the response, each showed an area of promise. The non-linear shear response matched the experimental response up to failure more accurately than any other model (Figure 7) up to approximately 1.4% strain. At this point, the model showed the wavy fibers had essentially straightened resulting in the increased stiffness indicated. Given this was not seen experimentally, the approach was deemed unsuccessful. Similarly, when cohesive elements were placed between the fiber tows, matrix damage was modeled, though the peak stress and strain were both under-predicted. Since neither was able to model the experimental damage progression, neither was used for additional cases (Table 4).

Based on the individual responses of these two techniques, a model was created placing cohesive elements between the fibers of the non-linear shear UMAT model. When used to model the initial IP wave case the response correlated to the experimental data. Specifically, the combined model curve and experimental IP wave curve had similar responses up to 0.5% strain as shown in Figure 7. Above this point the model under-predicted the peak stress, which was attributed to the uniformity of the model which was based on the average fiber misalignment angle. As such, the material failed through-the-thickness where all fibers were perfectly aligned, but the experimental specimen were not as consistent and some layers had a smaller fiber misalignment angle which increased the load carrying capability. Regardless, the combined model was within the acceptable range and matched strain at failure where the cohesive failures caused the sudden drop in load-carrying capability. Based on this result, additional correlations were attempted resulting in the best combination of accuracy, consistency, and predictive capability of all the modeling techniques tested (Table 4).

In summary, even though each model appeared to have different strengths, only the Hashin failure criteria and combined modeling techniques met the acceptable limits of the systematic approach employed. In both cases, this was true not only for the initial IP wave case, but also for additional wave and material cases (Table 4). After initial tuning of the damage parameters, the Hashin failure criteria model showed acceptable correlation in tension and moderate correlation in compression, while the combined model was acceptable for both. In tension, the combined model more accurately predicted both the initial stress-strain response and damage, even though the computational time was five times longer. when considering all cases, the combined approach was the found to be most the accurate, consistent, and predictive.

Wind Energ. Sci. Discuss., doi:10.5194/wes-2017-15, 2017
Manuscript under review for journal Wind Energ. Sci.
Discussion started: 12 April 2017

eawe european academy of wind energy
Open Access WIND ENERGY SCIENCE DISCUSSIONS

5 Conclusions & Future Work

To assess and predict the effects of manufacturing defects common to composite wind turbine blades, a comparison of several different damage progression models was performed resulting in several conclusions. Findings indicate that when material properties generated from unflawed material testing were used, all models were able to predict initial laminate stiffness when flaw geometries are discretely modeled. Models were run and a systematic approach was followed to assess the results compared to experimental results of flawed specimen. Specifically, the CDM using Hashin failure criteria was found to be accurate, consistent, and predictive particularly in tension for all wave and material cases once the damage properties were found. To account for the variations noted and improve the accuracy, a user-defined failure criteria was run, but results were not within the acceptable limits. Next, non-linear shear UMAT and cohesive element approaches were independently run. While each captured portions of the response, both resulted in unrealistic responses. However, when these two methods were combined, the result was the most accurate, consistent, and predictive correlation.

The results suggest these analytical approaches may be used to predict material response to possibly reduce material testing while also potentially supporting a probabilistic flaw framework. For this to be achieved, future work emphasized on scalability is necessary to be sure local defects are considered as part of entire structure. This requires development of a multi-scale approach which requires an understanding of flaw response when surrounded by unflawed material. Appropriate modeling of this response will allow for a better understanding of flaws on larger structures.

References

Abaqus Software and Abaqus Documentation: v. 6.12; Dassault Systemes Simulia Corp, Providence, RI, 2012.

Areias, P., & Belytschko, T. Analysis of three-dimensional crack initiation and propagation using the extended finite element method. *International Journal for Numerical Methods in Engineering*, *63*(5), 760-788, 2005.

Bouchard, P. O., Bay, F., Chastel, Y., & Tovena, I. Crack propagation modelling using an advanced remeshing technique. *Computer methods in applied mechanics and engineering*, *189*(3), 723-742, 2000.

Blackketter, D. M., Walrath, D. E., & Hansen, A. C. Modeling damage in a plain weave fabric-reinforced composite material. *Journal of Composites, Technology and Research*, *15*(2), 136-142, 1993.

Chaboche, J. L. A continuum damage theory with anisotropic and unilateral damage. *La Recherche Aérospatiale*, (2), 139-147, 1995.

Chang, F. K., & Chang, K. Y. A progressive damage model for laminated composites containing stress concentrations. *Journal of composite materials*, *21*(9), 834-855, 1987.

Chang, F. K., & Lessard, L. B. Damage tolerance of laminated composites containing an open hole and subjected to compressive loadings: Part I—Analysis. *Journal of Composite Materials*, *25*(1), 2-43, 1991.

Chapman D., John D. Whitcomb, C. Thermally induced damage initiation and growth in plain and satin weave carbon-carbon composites. *Mechanics of composite Materials and Structures*, *7*(2), 177-194, 2000.

Evcil, A. Simulation of Three Dimensional Progressive Damage in Composite Laminates. *Intl. Journal of Mechanics*, *2*, 2008.

Gorbatikh, L; D Ivanov, S Lomov, & I Verpoest. On modeling damage evolution in textile composites on meso-level via property degradation approach. Composites Part A, v38, n12, pp. 2433-2442, 2007.

Kachanov, L. M. Introduction. In *Introduction to continuum damage mechanics*. Springer Netherlands, 1986.

Karayev, K., Minguet, P., Lee, S., Balabanov, V., Muraliraj, N., Walker, T., ... & Robbins, D. Residual strength evaluation of typical aircraft composite structures with a large notch. In *53rd AIAA/ASME/ASCE/AHS/ASC Structures, Structural Dynamics and Materials Conference 20th AIAA/ASME/AHS Adaptive Structures Conference 14th AIAA*, p. 1862, 2012.

Krueger, R. Virtual crack closure technique: history, approach, and applications. *Applied Mechanics Reviews*, *57*(2), 109-143, 2004.

Lemanski, S. L., Wang, J., Sutcliffe, M. P. F., Potter, K. D., & Wisnom, M. R. Modelling failure of composite specimens with defects under compression loading. *Composites Part A: Applied Science and Manufacturing*, 48, 26-36, 2013.

Nelson, J., Cairns, D., Riddle, T., & Workman, J. Composite Wind Turbine Blade Effects of Defects: Part B-Progressive Damage Modeling of Fiberglass/Epoxy Laminates with Manufacturing Induced Flaws. In *53rd AIAA/ASME/ASCE/AHS/ASC Structures, Structural Dynamics and Materials Conference 20th AIAA/ASME/AHS Adaptive Structures Conference 14th AIAA*, p. 1421, 2012.

Nelson, J. W., Riddle, T. W., and Cairns, D. S.: Characterization and Mechanical Testing of Manufacturing Defects Common to Composite Wind Turbine Blades, Wind Energ. Sci. Discuss., doi:10.5194/wes-2017-13, in review, 2017.

Paquette, J. Blade Reliability Collaborative (BRC). *Sandia National Laboratories, Wind Energy Technology Dept*., 2012.

Tay, T. E., Tan, V. B. C., & Tan, S. H. N. (2005). Element-failure: an alternative to material property degradation method for progressive damage in composite structures. *Journal of composite materials*, *39*(18), 1659-1675.

Woo, K., Nelson, J., Cairns, D., & Riddle, T. (2013). Effects of Defects: Part B—Progressive Damage Modeling of Fiberglass/Epoxy Composite Structures with Manufacturing Induced Flaws Utilizing Cohesive Zone Elements. In *54th AIAA/ASME/ASCE/AHS/ASC Structures, Structural Dynamics, and Materials Conference* (p. 1628).